Differences in Structural Dynamics of Muscle and Yeast Actin Accompany Differences in Functional Interactions with Myosin†

Ewa Prochniewicz and David D. Thomas*

Department of Biochemistry, University of Minnesota Medical School, Minneapolis, Minnesota 55455

Received June 11, 1999; Revised Manuscript Received August 24, 1999

ABSTRACT: We have used spectroscopic probes ErIA and IAEDANS attached to Cys374 to compare the structural dynamics of yeast actin filaments with that of muscle actin, to understand the structural basis of the less productive interaction of yeast actin with myosin. Time-resolved phosphorescence anisotropy (TPA) of ErIA and steady-state fluorescence of IAEDANS were measured. TPA indicated more rapid rotational motion and more restricted angular amplitude in yeast actin. The fluorescence spectrum was less intense and more red-shifted in yeast actin, suggesting more exposure of the probe to solvent. These results indicate that the two actins differ substantially in the conformational dynamics of the C-terminal region. Binding of myosin S1 induced significantly different spectroscopic changes in TPA and fluorescence of muscle and yeast actin. As a result, the spectroscopic differences between the two actins were decreased by the addition of S1. These results suggest that yeast actin is less effective at activating myosin because of larger changes required in the structure of actin upon strong myosin binding. These results provide insight into the relationship between actomyosin dynamics and function, and they provide a useful framework for structure−function analysis of mutant yeast actin.

Actin is an essential component of the motile apparatus of muscle and nonmuscle cells. The X-ray crystal structures of skeletal muscle actin and the myosin head provided the foundation for studies on the relationship of structure and function in actin, suggesting hypotheses for localization of the binding sites between actin monomers in the filament and between actin and myosin (*1*, *2*). Strong biochemical support for these hypotheses was obtained from chemical cross-linking studies and through site-directed mutagenesis in actin from baker's yeast, which is a very useful organism for analysis of actin's function (*3*−*7*).

Yeast and muscle actin have about 87% sequence identity, and yeast actin displays all of actin's basic properties: polymerizes into double-stranded filaments, activates myosin ATPase, and moves in the in vitro motility assay. However, some properties differ quantitatively from the properties of muscle actin: yeast actin cannot be polymerized with KCl in the absence of $MgCl_2$, activates myosin ATPase with about twice higher K_m and about 5-fold lower V_{max}, and generates lower force in the in vitro motility assay (*8*, *9*). One of the possible explanations of this low catalytic efficiency of yeast actin is less negative charge at its N-terminus. The crystal structure of the acto-S1 complex and myosin mutagenesis data suggested that activation of myosin ATPase involves the interaction between negatively charged residues located between Asp1 and Asp25 and the lysine-rich 50-to-20 kD junction (*2*, *10*). The role of charges at the N-terminus was supported by the inhibitory effect of charge-to-alanine mutation Asp24Ala/Asp25Ala (*7*) and stimulatory effect of mutating the first yeast Met-Asp-Ser-Glu sequence to the muscle Asp-Glu-Asp-Glu sequence (*11*, *12*). The latter mutation decreased K_m to a similar level as that of muscle actin; however, V_{max} remained significantly lower, indicating that substitutions in other segments of the molecule are also functionally important.

Previous attempts to correlate amino acid substitutions with changes in actin's interaction with myosin were focused on nonskeletal muscle actins, such as smooth muscle actins from gizzard and aorta (*13*) and nonmuscle actin from *Acanthamoeba castellanii* (*14*). In contrast to yeast actin, these actins activate myosin ATPase with the same V_{max} as skeletal muscle actin, but they are similar to yeast actin in K_m about 2−3-fold higher than that for skeletal muscle actin. This increase in K_m smooth muscle actins was correlated with substitutions at the position 17 (skeletal Val to gizzard and aorta Cys) and 89 (skeletal Thr to gizzard and aorta Ser) (*13*). In yeast actin, as in both gizzard and *Acanthamoeba* actin, there is a substitution at position 17 (Val-Cys), but as in *Acanthamoeba*, there is no substitution at position 89. Concerning the extreme N-terminus, yeast's sequence (Met-Asp-Ser-Glu) differs from that of gizzard (absent-Glu-Glu-Glu) or *Acanthamoeba* actin (absent-Gly-Asp-Glu). The complexity of correlating changes in the actin-myosin interaction with specific sites of amino acid substitutions in actin's sequence is further indicated by different number of substitutions in each actin: 47 in yeast, 6 in gizzard, and 28 in *Acanthamoeba* (*15*−*17*).

Numerous spectroscopic studies indicated that functional interactions with myosin depend on local as well as global structure and dynamics of the actin filament. Changes in actin's dynamics upon binding of myosin heads were observed over a wide time range, from nanoseconds to

* To whom correspondence should be addressed. Telephone: (612)-625-2466. Fax: (612)624-0632. E-mail: ddt@ddt.biochem.umn.edu.

† This work was supported by a grant to E.P. from the Muscular Dystrophy Association and by a grant to D.D.T. from NIH (AR32961).

10.1021/bi991343g CCC: $18.00
Published on Web 10/23/1999

milliseconds (*18*−*21*). Direct observation under a fluorescence microscope (*20*) revealed that binding of myosin increases bending flexibility of the whole filament, and a model-based interpretation indicated that binding of myosin decreased the rates of internal motions in actin (*21*). The relationship between actin's structural dynamics and function was clearly demonstrated in several cross-linking studies, which inhibited sliding movement in the in vitro motility assay and significantly decreased the amplitude of the intrafilament rotational motions (*21*, *22*). In the present work, we continue testing the role of actin's dynamics and structure in functional interaction with myosin by doing comparative spectroscopic studies on muscle and yeast actin.

The microsecond-time-scale rotational motions were studied using transient phosphorescence anisotropy (TPA) of yeast and muscle actin labeled at Cys374 with a phosphorescent dye erythrosin iodoacetamide (ErIA). Model-based interpretation (*23*) of TPA allowed estimation of the total angular amplitude θ_c of the wobbling motions of the bound dye, orientation θ_a of the dye's absorption dipole relative to the filament axis, and torsional rigidity of the filament. Local structure of the C-terminal region in the two actin species was compared using static fluorescence measurements of actin labeled at Cys374 with a fluorescent dye IAEDANS.[1] The IAEDANS is an environmentally sensitive probe and in the past has been successfully applied for studies of the conformational changes in the skeletal muscle G-actin (*24*) as well as in the fluorescence energy transfer experiments to determine several distances within actin monomer and filament (*25*).

MATERIAL AND METHODS

Sample Preparation. Skeletal muscle actin was extracted from acetone powder of rabbit skeletal muscle with cold water, polymerized with 30 mM KCl for 1 or 2 h at room temperature, and centrifuged for 1 h at 200000*g*. The pellet was suspended in G-Ca buffer (5 mM Tris pH 7.5, 0.5 mM ATP, 0.2 mM $CaCl_2$), which additionally contained 1 mM DDT and 0.5 mM NaN_3, and dialyzed against the same buffer for 2 days at 4 °C. Actin was finally purified by chromatography on a Sephadex G-200 column eluted with 5 mM Tris pH 7.5, 0.2 mM $CaCl_2$, 0.2 mM ATP, and 0.5 mM NaN_3.

Wild-type yeast actin was isolated from baker's yeast and purified using DNase affinity column chromatography (*4*). One-fourth of a yeast cake was added to equal volume of Y-G-buffer (10 mM Tris pH 7.5, 0.2 mM $CaCl_2$, 0.2 mM ATP) with protease inhibitors: 20 μM PMSF and 10 μg/mL each of aprotinin, leupeptin, antipain, pepstatin, chymostatin, TLCK, TPCK, and BAAE. An equal volume of acid-washed glass beads was added, and the cells were lysed at 4 °C in a bead-beater by 12 cycles of beating: 20 s beating, followed by 3 min break. Cell debris were pelleted by 1 h centrifugation at 200000*g*, and the supernatant containing actin was applied on Affi-Gel DNase column equilibrated with Y-G-buffer with protease inhibitors. The column was sequentially washed with: Y-G-buffer with protease inhibitors, Y-G-buffer with 0.4 M NaCl, and with Y-G-buffer. The outlet of DNase column was then connected to small Whatman DE-52 column and actin was eluted directly on the DE-52 column with 50% formamide in Y-G-buffer. After exhaustive washing with Y-G-buffer, yeast actin was eluted from the DE-52 column with 0.3 M KCl in Y-G-buffer, dialyzed overnight against Y-G-buffer, polymerized with 1 mM $MgCl_2$ + 50 mM KCl, ultracentrifuged for 1 h at 200000*g*, and the pellets were suspended in G-Ca-buffer, the same as used during preparation of skeletal muscle actin.

Skeletal muscle and yeast actin was labeled with phosphorescent dye ErIA and fluorescent dye IAEDANS under the same conditions. The dye, freshly dissolved in DMF, was added to actin in G-Ca-buffer, and actin was immediately polymerized by adding buffer and salts; final concentrations were 240 μM dye, 24 μM actin, 20 mM Tris, pH 7.5, 1 mM $MgCl_2$, and 50 mM KCl. After 3 h incubation at 25 °C, the reaction was stopped by 10 mM DTT, actin was ultracentrifuged 1 h at 200000*g*, pellets were suspended in Mg-G-buffer (5 mM Tris pH 7.5, 0.2 mM $MgCl_2$, 0.5 mM ATP), and clarified by 10 min centrifugation at 300000*g*. Depolymerized actin was immediately polymerized with 1 mM $MgCl_2$ and 50 mM KCl, dialyzed overnight against 1 mM $MgCl_2$, 50 mM KCl, 10 mM Tris pH 7.5, and 0.2 mM ATP, and then ultracentrifuged 1 h at 200000*g*. The pellets were suspended in Mg-F-buffer: 3 mM $MgCl_2$, 10 mM Tris pH 7.5, with added 0.2 mM ATP. Complete removal of the free dye by this procedure was confirmed by precipitating the labeled actin with acetone, centrifuging the precipitate, and measuring the absorbance (538 nm) of the supernatant; no difference with a blank containing acetone only was found. The extent of labeling, expressed as mol dye/mol actin, was 0.6 ± 0.1 (muscle), 0.7 ± 0.1 (yeast) for ErIA, and 0.7 ± 0.2 (muscle), 0.9 ± 0.3 (yeast) for IAEDANS.

Myosin subfragment 1 (S1) was obtained by α-chymotrypsin digestion of myosin from rabbit skeletal muscle.

Actin-Activated S1 ATPase Assay. The ATPase reaction was measured in 3 mM $MgCl_2$, 10 mM Tris pH 7.5, and 3 mM ATP at 25 °C; increasing concentrations of S1 were added to 0.1 mg/mL actin. Control experiments confirmed a previous report (*26*) that at room temperature V_{max} and K_m of actin-activated ATPase measured at constant actin concentration and increasing S1 concentrations of S1 are the same as those measured at increasing concentrations of actin and constant concentration of S1. ATPase reaction was started by addition of ATP and terminated by 1.46% SDS. The amount of liberated P_i was determined using the method of Fiske and SubbaRow (*27*), and V_{max} and K_m were determined by fitting the ATPase rates to the Michaelis−Menten equation in the Origin5.0 program.

Protein Concentration. The concentration of unlabeled proteins was measured by ultraviolet absorption, assuming molar extinction coefficients of 0.63 mg mL^{-1} cm^{-1} for actin at 290 nm and 0.75 mg mL^{-1} cm^{-1} for S1 at 280 nm. The concentration of labeled actin was measured using the Bradford protein assay (*28*) with unmodified actin as a standard.

Spectroscopic Experiments. Skeletal muscle and yeast actin were stabilized against dilution-induced depolymerization by phalloidin added at 1:1 molar ratio. Control experiments

[1] Abbreviations and Textual Footnotes: ErIA, erythrosin iodoacetamide; IAEDANS, 5-((((2-iodoacetyl)amino)ethyl)amino)naphthalene-1-sulfonic acid; S1, myosin subfragment 1; TPA, transient phosphorescence anisotropy; PMSF, phenylmethanesulfonyl fluoride; TLCK, *N*-*p*-tosyl-L-lysine-chloromethyl ketone; TPCK, *N*-tosyl-L-phenylalanine chloromethyl ketone; BAAE, Nα-benzoyl-L-arginine ethyl.

confirmed that phalloidin protects yeast actin as well as muscle actin from depolymerization: dilution of the yeast actin−phalloidin complex (1:1) from 35 to 1.4 μM, as used in spectroscopic experiments, did not decrease the amount (98%) of sedimenting actin. For time-resolved phosphorescence anisotropy (TPA), phalloidin-stabilized F-actin was diluted in Mg-F-buffer (without ATP added) to 0.06 mg/mL, and for fluorescence measurement, actin was diluted in the same buffer to 0.1 mg/mL. Complexes of actin with S1 were preincubated at room temperature for 15−20 min to complete the hydrolysis of all ATP remaining in the actin sample, as determined by changes in light scattering intensity after addition of S1 to actin. Before TPA measurement, oxygen was removed by incubation with glucose oxidase (55 μg/mL), catalase (36 μg/mL), and glucose (45 μg/mL) (*29*). Fluorescence experiments did not require oxygen removal, as fluorescence intensity remained at a constant level during at least 30 min illumination by excitation light.

Transient Phosphorescence Anisotropy (TPA). TPA was measured as described previously (*23*). The actin-bound ErIA was excited with a 10-ns pulse of vertically polarized light at 540 nm, followed by detection of the time-dependent phosphorescence emission with a time resolution of 50 ns/channel. Phosphorescence signals were digitized with a transient recorder (dwell time 1 μs/channel resolution), and repeated transients were averaged by the microcomputer. The time-resolved phosphorescence was calculated as

$$r(t) = I_{vv}(t) - GI_{vh}(t)/I_{vv}(t) + 2GI_{vh}(t) \qquad (1)$$

where $I_{vv}(t)$ and $I_{vh}(t)$ are the vertically and horizontally polarized components of the emission signal. G is an instrumental correction factor, determined by performing the experiment with a solution of ErIA-labeled bovine serum albumin in 98% glycerol and adjusting G to give a final anisotropy value of zero, the theoretical value for an isotropically tumbling chromophore.

Anisotropy Data Analysis: (a) Model-Independent Fit to the Sum of Exponentials. The observed initial anisotropy $r_0 = r(t = 0)$, rotational correlation times Φ_i, amplitudes r_i, and the final anisotropy r_∞ were determined by fitting the anisotropy to a sum of n exponential terms and a constant:

$$r(t) = \sum_{i=1}^{n} r_i e^{-t/\Phi_i} + r_\infty \qquad (2)$$

The data were fitted in the 3−500 μs time range. The fit was judged to be optimal for a particular value of n if decreasing n made the fit worse and increasing n failed to improve it, as judged from the residuals (data minus fit) and χ^2. For the currently used samples, the fit was optimal for $n = 2$, with the residual not exceeding 1.5% of the maximum anisotropy. The observed initial anisotropy r_0 is lower than the theoretical maximum r_{max} by a factor $\kappa = r_0/r_{max} = S^2$-(ns), where S(ns) is the order parameter for nanosecond-time-scale rotational motions of the probe (*23*). The fitted final anisotropy r_∞ was within 10% of the calculated average $r(t)$ in the 400−500 μs time range, indicating that the decay reached a plateau level within the analyzed time window. Under this condition, $A_\infty = r_\infty/r_0 = S^2(\mu s)$, where $S(\mu s)$ is the order parameter for microsecond-time-scale rotational motion of the probe.

Table 1: Effect of ErIA and IAEDANS Labels in Muscle and Yeast Actin on Activation of S1 ATPase[a]

	muscle		yeast		
actin	V_{max}, s^{-1}	K_m, μM	V_{max}, s^{-1}	K_m, μM	relative efficiency
unlabeled	23.0 ± 1.9 (n = 4)	9.9 ± 2.7 (n = 4)	4.8 ± 0.3 (n = 3)	17.3 ± 5.6 (n = 3)	0.11 ± 0.10
ErIA	13.8 ± 1.4 (n = 3)	9.3 ± 2.0 (n = 3)	2.7 ± 0.3 (n = 2)	18.1 ± 4.4 (n = 2)	0.10 ± 0.03
IAEDANS	26.0 ± 2.4 (n = 3)	10.1 ± 0.5 (n = 3)	9.4 ± 0.7 (n = 3)	27.9 ± 7.6 (n = 3)	0.13 ± 0.04

[a] Data are expressed as means ± SD. Relative efficiency is the ratio of catalytic efficiency (V_{max}/K_m) of yeast actin to the catalytic efficiency of muscle actin.

(b) Model-Dependent Analyses. For the *wobble-in-cone* model, in which the emission transition moment of the probe is assumed to rotate isotropically within a cone of half-angle θ_c, the order parameter $S^2(\mu s)$ is given by (*30*):

$$A_\infty = r_\infty/r_0 = \left[\frac{1}{2}\cos\theta_c(1 + \cos\theta_c)\right]^2 \qquad (3)$$

For the model of a *segmented flexible cylinder*, with mean local cylindrical symmetry (*31*), we have shown previously (*23*) that the anisotropy decay of actin filaments is described by the formula:

$$r(t) = \kappa\left[A_0 + A_1 \exp\left(-\frac{1}{4}\sqrt{\frac{t}{\phi}}\right) + A_2 \exp\left(-\sqrt{\frac{t}{\phi}}\right)\right] \qquad (4)$$

The amplitudes A_i are functions of the angles θ_a and θ_e between the absorption and emission dipoles of the bound dye and the filament axis, $\varphi = (\pi a)^2 C\eta/4(k_B T)^2$, where a is the filament radius η is solvent viscosity and C is torsional rigidity of the filament. The anisotropy decays were fitted to eqs 2, 3, and 4 using a microcomputer. The data are shown in text as means ± SEM, with indicated number of measurements n.

Fluorescence. Fluorescence was measured at 25 °C in SPEX Fluorolog fluorimeter.

Reagents. The phosphorescence dye ErIA and fluorescence dye IAEDANS were purchased from Molecular Probes (Eugene, OR) and stored at −20 °C. Protease inhibitors, ATP, and phalloidin were obtained form Sigma (St. Louis, MO). All other chemicals were of reagent grade.

RESULTS

Effect of Labeling Muscle and Yeast Actin with ErIA and IAEDANS on the Activation of S1 ATPase. Early studies have shown that yeast actin is less efficient in activation of myosin ATPase than muscle actin (*8*, *12*), and this result has been confirmed in our present work. The ratio of relative catalytic efficiency V_{max}/K_m of yeast and muscle actin, 0.11 ± 0.1 (Table 1), is essentially the same as previously reported 0.12 (*12*). Labeling with ErIA decreased and with IAEDANS increased the activation of myosin ATPase, but the differences in the catalytic efficiencies of yeast and muscle actin were not significantly affected. Therefore, spectroscopic experiments are suitable for studies on the structural basis of the different functional interaction of the two actin species with myosin.

Microsecond-Time-Scale Dynamics of ErIA-Labeled Muscle and Yeast Actin Filaments. TPA of ErIA-labeled muscle and

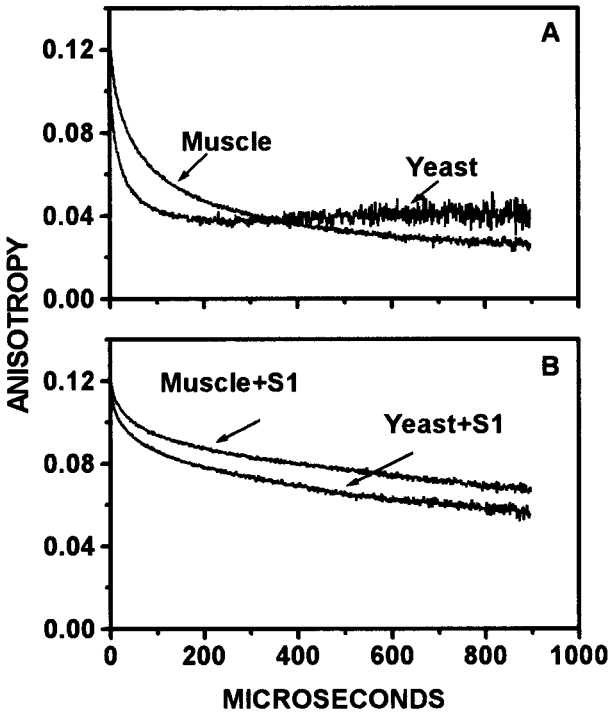

FIGURE 1: TPA of ErIA-labeled muscle and yeast actin in the absence (A) and presence (B) of S1 added at 1:1 molar ratio to actin. Actin concentration 0.06 mg/mL, 2 mM $MgCl_2$, 10 mM Tris pH 7.5, 25 °C.

yeast actin is shown in Figure 1A. TPA of muscle actin is the same as reported previously (*21*, *23*). In control experiments, we confirmed that different conditions of muscle actin polymerization (with 50 mM KCl in the absence of $MgCl_2$, as in refs *21* and *23*, and with 3 mM $MgCl_2$, as in the current work) have no effect on TPA. This indicates that the kind of tightly bound cation, Ca^{2+} or Mg^{2+}, has no effect on the microsecond-time-scale dynamics of actin. The TPA of yeast actin clearly differs from TPA of muscle actin, independently of the extent of labeling (from 0.2 to 0.8 mol of ErIA/mol of actin), and significant differences are in both rates of rotational motions and final anisotropy. The fit to a sum of two exponential terms (eq 2) showed that correlation times of rotational motions in yeast actin ($\Phi_1 = 10.6 \pm 0.7$ μs, $\Phi_2 = 77.8 \pm 9.6$ μs, $n = 16$) are about 2 times lower than in muscle actin (($\Phi_1 = 21.5 \pm 0.4$ μs, $\Phi_2 = 163.2 \pm 6.4$ μs, $n = 16$). This implies that the rates of the microsecond-time-scale motions are about 2 times higher; slightly lower (by less than 10%) r_0 of yeast actin indicates that submicrosecond-time-scale motions are also faster. Higher normalized final anisotropy A_∞ in yeast actin ($A_\infty = 0.375 \pm 0.004$, $n = 16$) resulted in the amplitude of wobbling motions $\theta_c = 44.3°$ (eq 3), which was about 6° smaller than the amplitude $\theta_c = 50.6°$ in muscle actin ($A_\infty = 0.267 \pm 0.007$, $n = 16$), indicating more restricted mobility of the labeled region.

The intrafilament dynamics of yeast and muscle actin was further analyzed by fitting TPA data to the torsional twist model (eq 4). According to the fit results, θ_a in yeast ($23.3 \pm 3.9°$, $n = 7$) was higher than in muscle actin ($16.0 \pm 0.2°$, $n = 8$), indicating that the absorption dipole of the bound ErIA forms a larger angle with the filament axis (*23*). The 5-fold lower time constant of torsional motions in yeast, $\varphi = 0.90 \pm 0.01$, $n = 7$, than in muscle, $\varphi = 4.9 \pm 0.3$, $n = 8$, indicated lower torsional rigidity C, i.e., higher flexibility of the yeast than muscle actin filaments. Since changes in all fit parameters except the angle between the absorption and emission dipoles of erythrosin were unrestricted, the obtained difference between θ_a and φ is underestimated suggesting that real differences can even be larger.

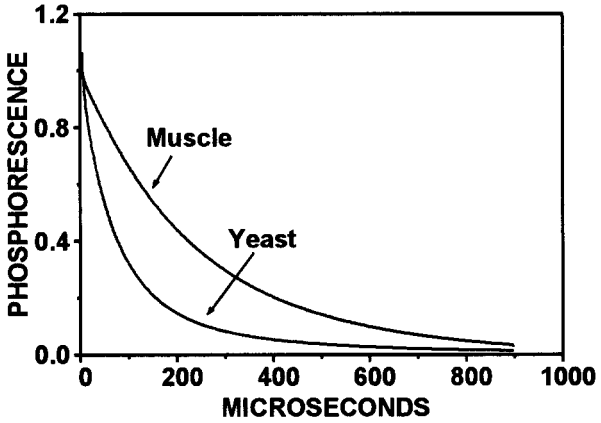

FIGURE 2: Decay of phosphorescence intensity of ErIA-labeled muscle and yeast actin. Experimental conditions as in Figure 1.

The above analysis of the anisotropy data indicated a significant difference in the structure (A_∞, θ_a) and dynamics (Φ_1, Φ_2, φ) of the C-terminus of the two actin species. This possibility was further assessed by analysis of the rates of phosphorescence intensity decay (Figure 2), which depend on the excited-state lifetime of the bound ErIA. The rate of the decay was much higher when ErIA was bound to yeast than muscle actin, and a fit of the intensity decay to the sum of two exponential terms resulted in different lifetimes. The lifetime in yeast actin, 98.3 ± 5.9 μs, $n = 8$, was about 2.4-fold shorter than in muscle actin, 237.9 ± 5.5 μs, $n = 8$, suggesting greater exposure of the dye to the quenching agents, most likely small amounts of oxygen in the buffer. Thus, the phosphorescence anisotropy and intensity data consistently indicate the differences in the dynamics/structure of the ErIA-binding region, i.e., the C-terminus, of yeast and muscle actin.

Effect of Strongly Bound S1 on the Microsecond-Time-Scale Dynamics of ErIA-Labeled Muscle and Yeast Actin Filaments. The interaction of actin with S1 was studied without removal of residual ATP from actin, which remained after suspending the pellets in Mg-F-buffer with 0.2 mM ATP. Control experiments have shown that removal of ATP from F-actin by suspending the pellets in the nucleotide-free F-buffer resulted in a substantial decrease of the initial anisotropy r_0, similar to that accompanying the decrease in the amount of tightly bound nucleotide and denaturation of actin. TPA measurements on acto-S1 were done after the residual ATP remaining in actin samples after dilution to the Mg-F-buffer (about 20 mM) was completely hydrolyzed by the added S1, as confirmed by light scattering measurements. Thus, the strongly bound acto-S1 complexes contained about a 10-fold molar excess of ADP over S1. A sedimentation assay showed that under our experimental conditions the strong binding of S1 to the labeled muscle and yeast actin was the same. The previously reported weaker binding of S1 to yeast than to skeletal actin was probably due to the presence of KCl in the buffer (*5*). Our control experiments showed that the addition of 0.1 M KCl to Mg-F-buffer

decreased the amount of S1 bound to yeast actin to from 91 to 74%, but had much less pronounced effect on binding to muscle actin (decrease from 94 to 89%).

Strong binding of S1 induced substantial changes in actin's phosphorescence anisotropy decay (Figure 1B). The principal effect was an increase in the final anisotropy r_∞, i.e., a decrease of the amplitude of rotational motions. However, the increase in the normalized final anisotropy $A_\infty = r_\infty/r_0$ in yeast, from 0.375 ± 0.004, $n = 16$ to 0.483 ± 0.015, $n = 13$ or about 1.3-fold, was less pronounced than about 2.2-fold increase in muscle actin, from 0.267 ± 0.007, $n = 16$ to 0.596 ± 0.018, $n = 11$. Binding of S1 also increased correlation times Φ_1 and Φ_2, and these changes were more pronounced in yeast (Φ_1 increased 2.4-fold, to 25.6 ± 1.8 μs, $n = 13$ and Φ_2 increased 5.1-fold, to 397.9 ± 41.9 μs, $n = 13$) than in muscle actin (Φ_1 increased 1.2-fold, to 24.8 ± 1.5 μs, $n = 11$ and Φ_2 increased 1.8-fold, to 289.3 ± 14.5 μs, $n = 11$). Fitting to the torsional twist model confirmed different extent of S1-induced changes in both actin species. The angles θ_a between the absorption dipole of ErIA and the filament axis became closer: $10.5 \pm 0.4°$, $n = 7$ in yeast and $8.4 \pm 0.7°$, $n = 6$ in muscle, and the difference between the time constants φ of the intrafilament motions decreased from 5-fold in free actins to 1.3-fold in acto-S1 complexes: 18.3 ± 2.8 μs, $n = 7$ in yeast and 15.4 ± 0.9 μs, $n = 6$; slightly higher φ in yeast actin indicates that in complex with S1 the yeast actin filaments became slightly more rigid than filaments of muscle actin. The decreases in θ_a confirmed our former conclusion (*21*) that the main effect of S1 is a shift of the C-terminus to the interior of the actin filament, and the present results indicate that this shift is more pronounced in yeast, about 13°, than in muscle actin, about 8°.

Strong binding of S1 to yeast and muscle actin increased the lifetime of the bound ErIA to 207.3 ± 3.0 μs, $n = 8$ in yeast and 350.7 ± 13.2 μs, $n = 7$ in muscle, suggesting a decrease in the exposure of the bound dye to quenching. However, the difference in the lifetimes of ErIA bound to the two actin species was smaller—1.7-fold—than that in the absence of S1, 2.4-fold. This result, consistent with phosphorescence anisotropy data, indicates that binding of S1 reduces structural differences in the C-terminal region of yeast and muscle actin.

Fluorescence Intensity of IAEDANS-Labeled Muscle and Yeast Actin. Fluorescence emission spectra of IAEDANS-labeled yeast and muscle actin are shown in Figure 3. The spectra differ in the position of the emission maximum, 475 nm for muscle IAEDANS−actin and 483 nm for yeast−IAEDANS−actin, and in the fluorescence emission intensities. We confirmed that this difference in intensities is not due to different concentration of the bound dye by direct comparison of the amount of IAEDANS label in the measured samples. Trypsin cleavage of the labeled C-terminus, followed by ultracentrifugation of the cleaved sample showed that more than 90% of the label was released from actin. The fluorescence intensity of IAEDANS bound to the cleaved C-terminus is independent of the environment in the protein, so the ratio of intensities of trypsin-treated IAEDANS-yeast and muscle actin is equal to the ratio of the amount of the bound label. Normalization of fluorescence spectra of IAEDANS-labeled−actins to this ratio showed that the maximum intensity of IAEDANS−yeast−actin was

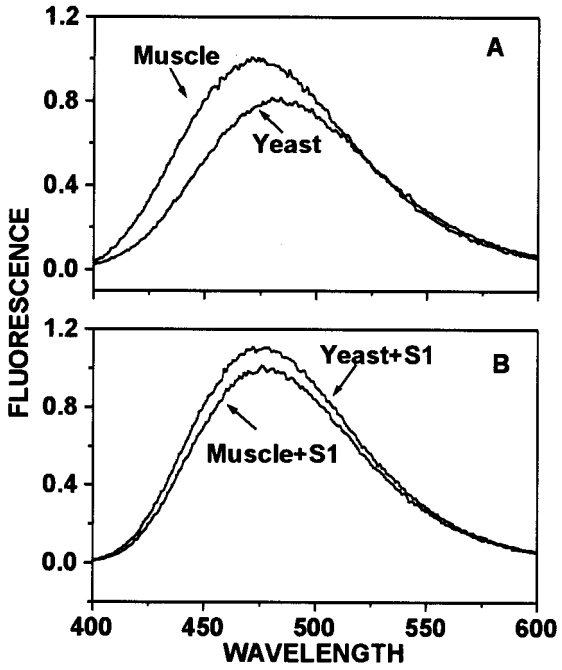

FIGURE 3: Fluorescence emission spectra of IAEDANS-labeled muscle and yeast actin in the absence (A) and presence of S1 (B) added at 1:1 molar ratio. The spectra were recorded with $\lambda_{exc} = 345$ nm and normalized to (a) the amount of actin-bound IAEDANS determined using trypsin digestion (as described in the text) and (b) the maximum emission intensity of IAEDANS-labeled muscle actin, taken as the average of intensities at 474, 475, and 476 nm. Actin concentration 0.1 mg/mL, 3 mM $MgCl_2$, 10 mM Tris pH 7.5, 25 °C.

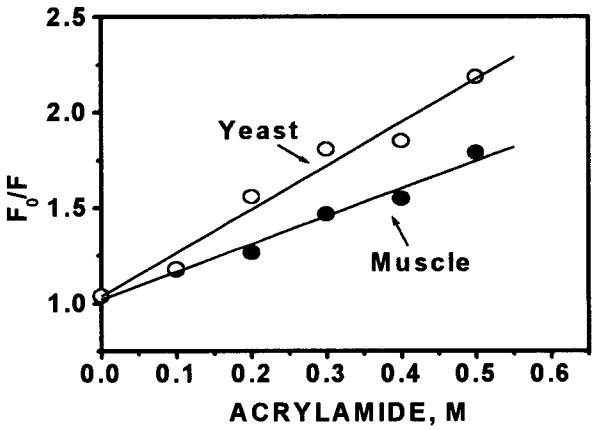

FIGURE 4: Quenching of fluorescence emission intensity of IAEDANS-labeled muscle and yeast actin by increasing concentrations of acrylamide. The fluorescence emission intensity was recorded before and after addition of increasing concentrations of acrylamide, with $\lambda_{exc} = 345$ nm and $\lambda_{em} = 475$ nm for muscle and 483 nm for yeast actin. Straight line represents the fit to Stern−Volmer equation. Other experimental conditions as in Figure 3.

0.7 ± 0.02 (SEM, $n = 6$) of that of muscle actin. This about 30% lower intensity and red shift of fluorescence maximum indicates that the yeast−actin-bound IAEDANS could be more exposed to the environment than IAEDANS bound to muscle actin.

This interpretation of the difference in fluorescence emission spectra of yeast and muscle actin was supported by measuring quenching of the fluorescence of actin-bound IAEDANS by acrylamide (Figure 4). The data fitted to Stern−Volmer equation gave higher quenching constants K_Q for IAEDANS−yeast (2.27 ± 0.2 M^{-1}) than for IAEDANS−

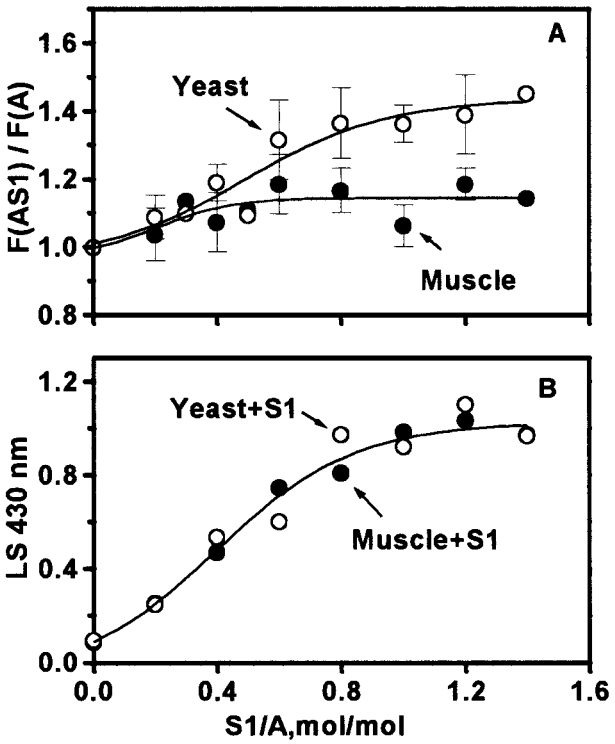

FIGURE 5: The effect of S1 on fluorescence emission (A) and on light scattering (B) of IAEDANS-labeled muscle and yeast actin. (A) The effect of S1 on fluorescence emission intensity was expressed as the ratio F(AS1)/F(A), where F(AS1) and F(A) are the fluorescence emission intensities of acto-S1 complexes before and after dissociation by 3 mM ATP + 0.1 M KCl, respectively; each data point in (A) represents average ± SD ($n = 3$). λ_{exc} = 345 nm, λ_{em} = 475 nm (muscle), and 483 nm (yeast), actin 0.1 mg/mL, 3 mM $MgCl_2$ 10 mM Tris pH 7.5. The curves represent fit to the "sigmoidal growth" function. (B) The binding of S1 to IAEDANS-labeled muscle and yeast actin measured by light scattering at 430 nm; other experimental conditions as in (A).

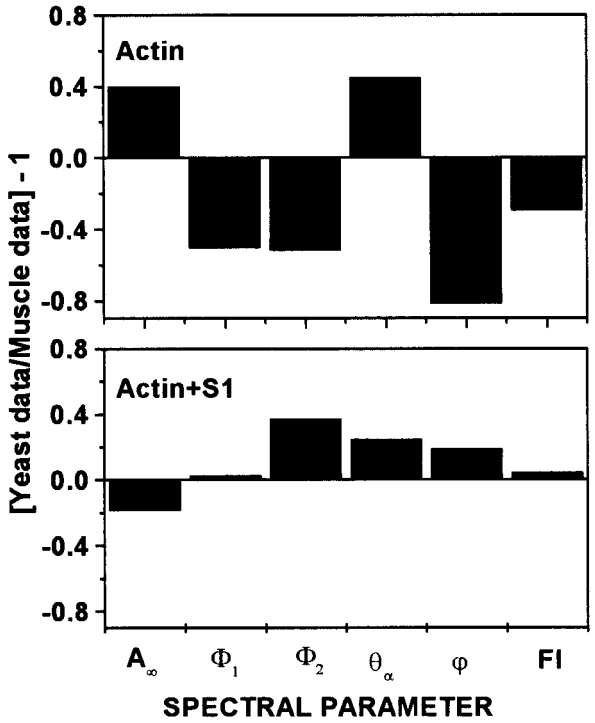

FIGURE 6: Comparison of spectral parameters of ErIA and IAEDANS-labeled muscle and yeast actin in the absence (actin) and the presence (actin + S1) of S1. Yeast data/muscle data is the ratio of each spectral parameter for muscle and yeast actin. The positive values of ([yeast/muscle data] − 1) are for parameters that are larger, and the negative values are for the parameters that are smaller for yeast than muscle actin. The parameters: final anisotropy A_∞, correlation times of the microsecond-time-scale rotational motions Φ, the orientation of the emission dipole of ErIA relative to the filament axis θ_a, the time constant of torsional motions φ, and fluorescence intensity FI are indicated in the text.

muscle-actin (1.45 ± 0.1 M^{-1}), which indicates that yeast actin-bound IAEDANS is more accessible to collisional quenching than that bound to muscle actin.

Effect of Strongly Bound S1 on the Fluorescence Intensity of IAEDANS-Labeled Muscle and Yeast Actin. The effect of S1 on actin's fluorescence intensity was expressed as the ratio of emission intensities of acto-S1 before and after dissociation by 3 mM ATP + 0.1 M KCl. The changes in actin's fluorescence upon dissociation were not caused by changes in the turbidity. Control experiments with unlabeled acto-S1 and cysteine-bound IAEDANS (to prevent its reaction with SH groups of actin or S1) showed that IAEDANS fluorescence emission is not affected by the 10-fold turbidity decrease upon dissociation of the acto-S1 by 2 mM ATP + 0.1 M KCl.

The binding of S1 increased the emission intensity of IAEDANS−muscle-actin by about 14% without shifting its maximum (Figure 5A), in agreement with the previously reported data (*32*). The increase in the emission intensity of IAEDANS-labeled yeast actin was much more pronounced, by about 40%, and the fluorescence emission spectra of both actin species in a strong complex with S1 become similar, differing in intensities only by about 5%. Binding of S1 to yeast actin was also accompanied by a blue shift of the maximum, from 483 to 475 nm. The data in Figure 5B show that binding of S1 to muscle and yeast actin, measured by increase in light scattering at 430 nm, is the same. Thus, the difference in the effect of S1 on fluorescence intensity cannot be due to the difference in binding to the two actin species, but indicates a difference in the extent of structural changes.

Data Summary. The differences in spectral properties of muscle and yeast actin in the presence and absence of S1, indicated numerically in the text, are illustrated in Figure 6. If the spectral parameters of yeast and muscle actin were equal for both actin species, then the ratio (yeast data/muscle data) would be 1, and the difference ([yeast data/muscle data] − 1), indicated on the vertical axis, would be zero. However, the large bars on the figure show that it is not the case. Furthermore, the comparison of the size of the bars on the upper (actin) and lower (actin + S1) panel clearly shows that the difference between each spectral parameter for yeast and muscle actin significantly decreased when actin was bound to S1. This suggests that activation of S1 ATPase by yeast actin is accompanied by structural changes, which create muscle−actin-like contact sites at the interface between interacting actin and myosin.

DISCUSSION

Spectroscopically Detected Differences between Muscle and Yeast Actin. Phosphorescence and fluorescence data consistently indicated that yeast actin differs significantly from muscle actin in the structure/dynamics of the C-terminus. The differences in the phosphorescence and

fluorescence quenching and red shift in the fluorescence emission indicated that the yeast actin's C-terminus is more exposed to the environment than that of muscle actin. This conclusion is consistent with the observation that yeast actin shows a smaller increase in the fluorescence intensity of pyrene at Cys374 during polymerization (*9*).

Relationship between the Differences at the C-Terminus and the Structure of the Actin Monomer and Filament. The spectroscopic difference between yeast and muscle actin could result from structural alterations induced by amino acid substitutions close to the labeled Cys374. In the muscle actin sequence, the substitutions nearest to Cys374 are in positions 372, 365, and 350 (*15*) and their distances to Cys374 (about 11.9, 12.7, and 22.1 Å, respectively) are comparable to the maximum dimension of the spectroscopic probes ErIA and IAEDANS, 13.9 and 12.5 Å. However, the differences could also reflect allosteric transfer of changes from distant regions of actin monomer, such as subdomain 2 and the nucleotide binding cleft (*33*−*35*). In yeast actin, these regions had different structure than in muscle actin, as indicated by faster subtilisin cleavage between Met47 and Gly48 and 5-fold higher rate of nucleotide exchange (*9*, *36*).

The importance of the C-terminus for structural integrity of F-actin (*34*−*38*) suggests that spectral differences detected in this region could also reflect global structural differences between the filaments. For example, assuming that filaments are homogeneous flexible rods, the difference in the microsecond-time-scale dynamics was interpreted as higher torsional flexibility of yeast actin (Figure 1). Higher flexibility of yeast F-actin has been previously suggested as an explanation for its greater fragmentation in the in vitro motility assay (*9*) and more rapid binding of phalloidin rhodamin (*39*).

Suggested differences in the structure and dynamics of actin filaments are supported by the 3D-reconstructions from electron micrographs of negatively stained filaments. Yeast F-actin had less connectivity between two long-pitch strands of the filament as well as within the same strand and similarity of yeast actin filaments to muscle F-actin with two or three C-terminal residues cleaved by trypsin indicated that the state of its C-terminus is altered (*34*, *40*). Further contributions to different structure of the two filaments could come also from several amino acid substitutions in the proposed regions of intermonomer interactions, as previously indicated (*39*).

Possible Functional Role of S1-Induced Changes in the Structure and Dynamics of Muscle and Yeast Actin. Our previous work (*21*) indicated that inhibition of functional actin-myosin interactions by structural perturbations of actin could be related to the restrictions of the microsecond-time-scale motions within the filament. The present phosphorescence data support such a possibility; yeast actin, which is less efficient in activation of myosin ATPase, had more restricted amplitude of intrafilament wobbling motions, and its A_∞ was less affected by S1 binding than that of muscle actin (Figure 1). The difference in the effect of S1 on yeast and muscle actin was detected also in fluorescence experiments, but in this case the effect of S1 on emission intensity of yeast actin was larger than that of muscle actin. However, it is possible that phosphorescence and fluorescence labels may report different extent of changes. Since ErIA and IAEDANS have different effects on myosin binding sites, as indicated by their opposite effect on activation of S1 ATPase (Table 1), binding of S1 to these sites could have different effects on the two dyes.

The quantitative difference between yeast and muscle actin in the extent of S1-induced changes in both phosphorescence and fluorescence (Figure 6) is in sharp contrast with the previous spectroscopic studies on cardiac skeletal and smooth muscle actins where the fluorescence, EPR, and ST-EPR did not find essential structural differences in the absence as well as in the presence of myosin heads (*13*, *41*). One of the possible explanations is that such similarity between muscle actins reflects similarity of their main function, which is contractility. Smooth muscle actins are identical in the in vitro motility assay and V_{max} of actin-activated myosin ATPase with skeletal muscle actin (*42*, *43*), and the differences in the actomyosin ATPases of smooth and skeletal muscle were traced to different properties of myosins. On the other hand, yeast actin is a component of the yeast cytoskeleton; it could interact with yeast myosin II, supposedly in the process of vesicles movement (*44*), but also its main function could be related to the dynamics of the cytoskeleton via interaction with many actin-binding proteins. Consequently, the structure of the proposed sites of interaction with myosin, which are close to the sites of interactions with actin-binding proteins such as fimbrin (*45*), could be altered for effectiveness of yeast's actin intracellular functions and result in altered interaction with skeletal muscle myosin. The comparison of amino acid sequences shows substitutions not only in the regions of weak electrostatic interactions with myosin at the N-terminus, but also in the regions of strong stereospecific interactions (positions 144 and 350). The structure of myosin binding sites could be also affected through allosteric coupling to structurally different C-termini; such coupling is suggested by inhibitory effect of removal of two C-terminal residues of muscle actin on V_{max} of actin-activated ATPase (*38*).

It is commonly proposed that the fundamental structural change in the acto-myosin interaction is the change in myosin structure from a weak-binding to a strong-binding state (*46*). The studies on a limited number of nonskeletal muscle actins, *which did not include yeast actin*, led to the conclusion that *all* actins activate myosin ATPase with the same V_{max} (*47*). This was regarded as a strong support for the model of contractility where the rate-limiting step in the hydrolysis of ATP by actomyosin is a change in myosin conformation that is independent of actin. The studies on yeast actin clearly show that V_{max} of the actomyosin ATPase can be dependent on actin species, and, therefore, actin should be regarded as an active component of the contraction process. Since actin undergoes a structural change upon strong myosin binding (*18*−*21*), it is also likely that the effectiveness of actin depends on its ability to undergo this structural transition. Preliminary experiments indicated that in contrast to strongly binding, weak interactions (according to turbidity measurements 20−40% of actin was bound to S1 in the presence of ATP) did not have a significant effect on the fluorescence intensities of the IAEDANS-labeled yeast actin. This is consistent with results obtained for pyrene labeled muscle actin where about 70% saturation with weakly bound S1 did not affect fluorescence (*48*). We suggests that the lesser effectiveness of yeast actin, compared to muscle actin, is related to its different structural dynamics and the larger

structural transition which accompanies its strong interaction with myosin.

ACKNOWLEDGMENT

The authors thank Dr. P. Rubenstein for help with purification procedure of yeast actin and R. Bennet for technical assistance.

REFERENCES

1. Holmes, K., Popp, D., Gebhard, W., and Kabsch, W. (1990) *Nature 347*, 44−49.
2. Rayment, I., Holden, H. M., Whittaker, M., Yohn, C. B., Lorenz, M., Holmes, K. C., and Milligan, R. A. (1993) *Science 261*, 58−64.
3. Mornet, D., Bertrand, R., Pantel, P., Audemard, E., and Kassab, R. (1981) *Nature 292*, 301−306.
4. Cook, R. K., Blake, W. T., and Rubenstein, P. (1992) *J. Biol. Chem. 267*, 9430−9436.
5. Miller, C., and Reisler, E. (1995) *Biochemistry 34*, 2694−2700.
6. Miller, C. J., Doyle, T. C., Bobkova, E., Botstein, D., and Reisler, E. (1996) *Biochemistry* 35, 3670−3676.
7. Miller, C. J., Wong, W. W., Bobkova, E., Rubenstein, P. A., and Reisler, E. (1996) *Biochemistry 35*, 16557−16565.
8. Buzan, J. J., and Frieden, C. (1996) *Proc. Natl. Acad. Sci. U.S.A. 93*, 91−95.
9. Kim, E., Miller, C. J., and Reisler, E. (1996) *Biochemistry 35*, 16566−16572.
10. Uyeda, T. Q. P., Ruppel, K. M., and Spudich, J. A. (1994) *Nature 368*, 567−569.
11. Wong, W. W., Doyle, T. C., and Reisler, E. (1999) *Biochemistry 38*, 1365−1370.
12. Cook, R. K., Root, D., Miller, C., Reisler, E., and Rubenstein, P. (1993) *J. Biol. Chem. 268*, 2410−2415.
13. Mossakowska, M., and Strzelecka-Golaszewska, H. (1985) *Eur. J. Biochem. 153*, 373−381.
14. Gordon, D. J., Eisenberg, E., and Korn, E. D. (1976) *J. Biol. Chem. 251*, 4778−4786.
15. Wertman, K. W., Drubin, D. G., and Botstein, D. (1992) *Genetics 132*, 337−350.
16. Vandekerckhove, J., Lal, A. A., and Korn, E. D. (1984) *J. Mol. Biol. 172*, 141−147.
17. Vandekerckhove, J., and Weber, K. (1978) *Proc. Natl. Acad. Sci. U.S.A. 75*, 1106−1110.
18. Miki, M., Wahl, P., and Auchet, J. C. (1982) *Biochemistry 21*, 3661−3665.
19. Kouyama, T., and Mihashi, K. (1980) *Eur. J. Biochem. 105*, 29−287.
20. Yanagida, T., Nakase, M., Nishiyama, K., and Oosawa, F. (1984) *Nature 307*, 58−60.
21. Prochniewicz, E., and Thomas, D. D. (1997) *Biochemistry 36*, 12845−12853.
22. Kim, E., Bobkova, E., Miller, C. J., Orlova, A., Hegyi, G., Egelman, E., Muhlrad, A., and Reisler, E. (1998) *Biochemistry 37*, 17801−17809.
23. Prochniewicz, E., Zhang, Q., Howard, E., and Thomas, D. D. (1986) *J. Mol. Biol. 255*, 446−457.
24. Frieden, C., Lieberman, D., and Gilbert, H. R. (1980) *J. Biol. Chem. 255*, 8991−8993.
25. dos Remedios, C. G., Miki, M., and Barden, J. (1987) *J. Muscle Res. Cell Motility 8*, 97−117.
26. Wagner, P. D., and Weeds, A. (1979) *Biochemistry 18*, 2260−2266.
27. Fiske, C. H., and SubbaRow, Y. (1925) *J. Biol. Chem. 66*, 375−400.
28. Bradford, M. M. (1976) *Anal. Biochem. 72*, 248−254.
29. Eads, T. M., and Thomas, D. D. (1984) *J. Mol. Biol. 179*, 55−81.
30. Kinoshita, K., Kawato, S., and Ikegami, A. (1977) *Biophys. J. 20*, 289−305.
31. Schurr, J. M. (1984) *Chem. Phys. 84*, 71−96.
32. Moens, P. D. J., and dos Remedios, C. G. (1997) *Biochemistry 36*, 7353−7360.
33. Crosbie, H. R., Miller, C., Cheung, P., Goodnight, T., Muhlrad, A., and Reisler, E. (1994) *Biophys. J. 67*, 1957−1964.
34. Orlova, A., and Egelman, H. E. (1995) *J. Mol. Biol. 245*, 582−597.
35. Moraczewska, J., Strzelecka-Golaszewska, H., Moens, P. D. J., and DosRemedios, C. G. (1996) *Biochem. J. 317*, 605−611.
36. Miller. C. J., Cheung, P., White, P., and Reisler, E. (1995) *Biophys. J. 68*, 50−54.
37. Strzelecka-Golaszewska, H., Mossakowska, M., Wozniak, A., Moraczewska, J., and Nakayama, H. (1995) *Biochem. J. 307*, 527−534.
38. O'Donoghue, S. I., Miki, M., and dosRemedios, C. G. (1992) *Arch. Biochem. Biophys. 293*, 110−116.
39. DeLaCruz, E. M., and Pollard, T. D. (1996) *Biochemistry 35*, 14054−14061.
40. Orlova, A., Chen, X., Rubenstein, P., and Egelman, E. H. (1997) *J. Mol. Biol. 271*, 235−243.
41. Mossakowska, M., Belagyi, J., and Strzelecka-Golaszewska, H. (1988) *Eur. J. Biochem. 175*, 557−564.
42. Harris, D. E., and Warshaw, D. M. (1993) *Circulation Res. 72*, 219−224.
43. Prochniewicz, E., and Strzelecka-Golaszewska, H. (1980) *Eur. J. Biochem. 106*, 305−312.
44. Johnston, G., Prendergast, J., and Singer, R. (1991) *J. Cell. Biol. 113*, 539−551.
45. Hanein, D., Matsuidara, P., and DeRosier, D. J. (1997) *J. Cell Biol. 139*, 387−396.
46. Eisenberg, E., and Hill, T. (1985) *Science 227*, 999−1006.
47. Korn, E. D. (1978) *Proc. Natl. Acad. U.S.A. 75*, 588−599.
48. Geeves, M. A., Jeffries, T. E., and Millar, N. C. (1986) *Biochemistry 25*, 8454−8458.

BI991343G